J|A|C|S COMMUNICATIONS

Published on Web 10/30/2009

Nanopore Extrusion-Induced Transition from Spherical to Cylindrical Block Copolymer Micelles

Qianjin Chen,[†] Hong Zhao,[†] Tian Ming,[‡] Jianfang Wang,*[,‡] and Chi Wu*[,†]

Department of Chemistry and Department of Physics, The Chinese University of Hong Kong, Shatin, Hong Kong SAR, China

Received September 17, 2009; E-mail: chiwu@cuhk.edu.hk; jfwang@phy.cuhk.edu.hk

Cylindrical micelles made of soluble and insoluble segments have been attracting increasing attention owing to their many interesting applications. They can function as templates to align inorganic nanocrystals into one-dimensional arrays[1] and fabricate polymer−silica[2] and polymer−metal oxide nanowires.[3] Cylindrical micelles containing peptides have been shown to be able to direct the mineralization of hydroxyapatite with controlled crystalline orientations[4] and induce rapid differentiation of neural progenitor cells.[5] Moreover, cylindrical micelles are also useful for sustained drug release.[6] They have been demonstrated to persist in the circulation up to one week after intravenous injection, which is about 10 times longer than the corresponding spherical ones.[7]

The formation of cylindrical micelles has typically been realized by designing the molecular structures and varying the molecular weights of the soluble and insoluble segments.[8] The transition from spherical to cylindrical micelles can also be induced by changing the solvent and temperature. Moreover, some unconventional means for the preparation of cylindrical micelles have recently been demonstrated, including kinetic control,[9] the use of interfacial instabilities,[10] and aromatic oxidation.[11] Herein we report on a new and facile method for transforming spherical to cylindrical micelles. The transformation is achieved by extruding the spherical micelles through nanoscale pores (Figure 1a). The extrusion process allows for continuous and large-scale production of cylindrical micelles.

We used polystyrene-*b*-polyisoprene (PS_{170}-*b*-PI_{140}) diblock copolymer with a polydispersity index of 1.06.[12,13] We previously measured the force required to pull individual chains out of each spherical micelle formed in pure *n*-hexane.[13] In this experiment, the copolymer was first dissolved in tetrahydrofuran (THF). *n*-Hexane was then added dropwise under stirring until the concentration of THF was reduced to 2.8 vol%. The final concentration of the copolymer was 5×10^{-4} g/mL. The copolymer solution was kept at room temperature for more than 3 months before use. Our extrusion setup is composed of an SGE gastight syringe and a Whatman 10-mm-diameter membrane. The membrane has a double layer structure.[13,14] One layer is 59-μm thick and contains 200-nm pores, and the other layer is 1-μm thick and contains 20-nm pores. On average, each small pore is covered by a large pore, with a pore density of $\sim 5 \times 10^8$ cm^{-2}. During the extrusion operation, the membrane was positioned with the large-pore layer facing the incoming solution. The flow rate of the copolymer solution through the membrane was controlled with a Harvard PHD 2000 syringe pump. The extrusion was performed at room temperature. The variation of temperature will alter the solvent quality. Our results show that the workable range for the extrusion to produce cylindrical micelles is ~2−6 vol% of THF. If the interaction of the PS blocks in the core is too strong, it will be difficult to push the spherical micelles through the nanopores. If the interaction is too weak, no spherical micelles will be formed.

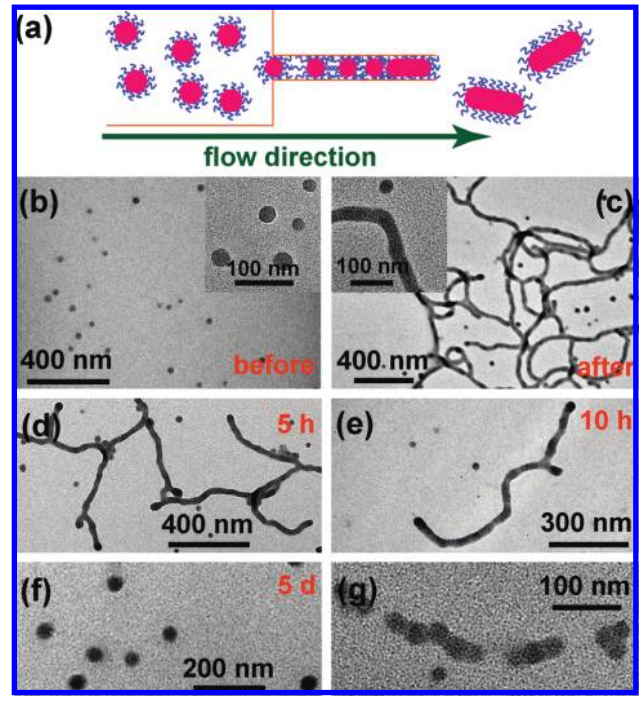

Figure 1. (a) Schematic showing the extrusion process. (b) TEM (FEI CM120) image of the micelles before the extrusion. (c) TEM image of the micelles obtained after the extrusion. The insets are the corresponding zoomed-in images (FEI Tecnai T20). (d−f) TEM images of the micelles obtained at 5 h, 10 h, and 5 d, respectively, after the extrusion. (g) High-magnification TEM image acquired right after the extrusion. The flow rate of the copolymer solution is 40 mL/h. The micelle solutions were directly dropcast on carbon film-supported copper grids and dried in air.

Transmission electron microscopy (TEM) imaging was performed to characterize the copolymer micelle morphologies. Figure 1b shows a representative TEM image of the micelles formed in the initial solution. All of the micelles are spherical. After the micelle solution was extruded through the membrane, a number of cylindrical micelles were observed (Figure 1c). They are entangled together, with lengths of up to several micrometers. The average diameters of the spherical and cylindrical micelles measured from their high-magnification TEM images (Figure 1b,c, insets) are (28 ± 5) and (33 ± 4) nm, respectively. They are nearly the same within the experimental uncertainties.

Dynamic light scattering (DLS) was also carried out to probe the copolymer micelles. An ALV 5022F spectrometer equipped with a time correlator and a He−Ne laser (632.8 nm, 22 mW) was used. The scattering signal was detected at an angle of 20°. From each measured intensity−intensity time correlation function, a hydro-

[†] Department of Chemistry.
[‡] Department of Physics.

10.1021/ja907898u CCC: $40.75

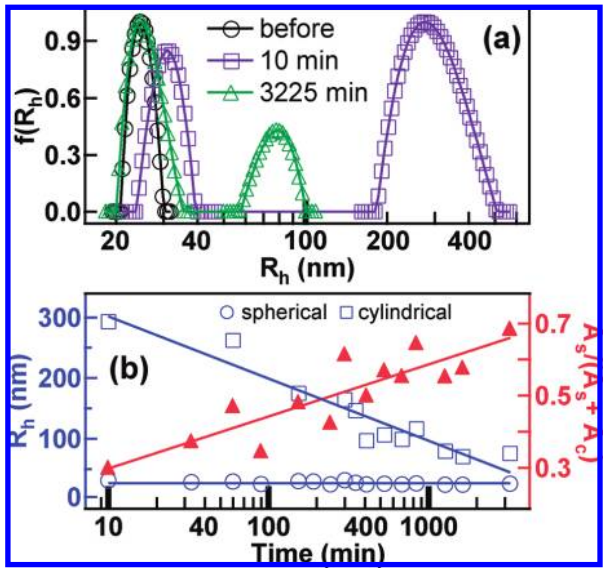

Figure 2. (a) Normalized hydrodynamic radius distributions $f(R_h)$ obtained before and at 10 and 3225 min after the extrusion. The solution flow rate is 40 mL/h. (b) Left axis: dependence of the hydrodynamic radii of the spherical (circles) and cylindrical (squares) micelles on the elapsed time after the extrusion. Right axis: dependence of the contribution of the spherical micelles (triangles) on the elapsed time. A_s and A_c are the peak areas of the spherical and cylindrical micelles on the $f(R_h)$ plots, respectively. The lines are guides to the eye.

dynamic radius distribution $f(R_h)$ can be obtained.[13] The relative peak area changes on $f(R_h)$ can approximately reflect the changes in the relative amounts of different scattering objects. Figure 2a shows the $f(R_h)$ curves obtained before (black) and after (purple) the extrusion. Only one peak is present before the extrusion. The hydrodynamic radius at the peak maximum is 25 nm (Supporting Information). The shell thickness and the core radius are estimated to be 13 and 12 nm, respectively.[15] This peak corresponds to the spherical micelles. In contrast, two peaks are present after the extrusion. One is peaked at 31 nm and narrow, and the other is centered at 275 nm and broad. According to the TEM observations (Figure 1b,c), these two peaks correspond to the spherical and cylindrical micelles, respectively. Because of their entanglement and large length distribution, the scattering peak associated with the cylindrical micelles is relatively broad.

The diameter of the small pores of the membrane is smaller than that of the spherical micelles. During the extrusion process, the spherical micelles are squeezed into the nanopores by the flowing liquid. The confinement in the nanopores induces the fusion of the spherical micelles into the cylindrical ones, which are thereafter pushed out of the nanopores (Figure 1a). This extrusion process was found to show a dependence of the relative amounts of the cylindrical versus spherical micelles on the flow rate (Figure S1, Supporting Information). The fraction of the peak area of the cylindrical micelles increased as the flow rate was raised. It saturated above a flow rate of 10 mL/h. The flow rate at which the saturation occurred is believed to be dependent on the relative sizes between the spherical micelles and the nanopores.

The mixture solvent used in our experiments is thermodynamically favorable for the formation of the spherical micelles. The cylindrical micelles formed through the extrusion changed gradually into the spherical micelles. This transformation was monitored with DLS (Figure 2) and TEM (Figure 1 and Figure S2, Supporting Information). The hydrodynamic radius of the cylindrical micelles decreased from 300 to 70 nm within 2 d after the extrusion, while that of the spherical micelles stayed at ~27 nm. The contribution of the spherical micelles to the total scattering signal increased steadily as a function of time (Figure 2b). TEM imaging shows the undulation in diameter along the length axis of the cylindrical micelles. The undulation evolved into pearl-necklace-like nanostructures and then into spherical micelles (Figure 1g). The entire transformation process was complete after ~5 d. In addition, most cylindrical micelles possess thicker spherical end caps (Figure 1d). In comparison, the spherical end caps are observed to be similar in diameter to the cylindrical micelles in a previous study with PS-*b*-PI copolymers,[16] where the morphological change is induced by the change in temperature and thus the solvent quality. In our experiments, the solvent quality remained constant before and after the extrusion. Further studies are required to understand the transformation process in our experiments.

In conclusion, nanopore extrusion-induced transition from spherical to cylindrical micelles has been demonstrated. The production of cylindrical micelles using this extrusion process is continuous, simple, and scalable. We are going to apply this preparation method to other block copolymers and develop methods for cross-linking the cylindrical micelles[17] into nanofibers during their production. We believe our method will open enormous opportunities for the applications of copolymer nanofibers in composite materials and biotechnology.

Acknowledgment. This work was supported by an NNSFC Key Project (20934005) a RGC grant (Reference Number, CUHK4037/07P; Project Code, 2160331). We thank Liangzhi Hong for assistance with the nanopore extrusion.

Supporting Information Available: The diffusion coefficients, $f(R_h)$ plots, and TEM images of the micelles. This material is available free of charge via the Internet at http://pubs.acs.org.

References

(1) (a) Wang, H.; Wang, X. S.; Winnik, M. A.; Manners, I. *J. Am. Chem. Soc.* **2008**, *130*, 12921–12930. (b) Wang, H.; Lin, W. J.; Fritz, K. P.; Scholes, G. D.; Winnik, M. A.; Manners, I. *J. Am. Chem. Soc.* **2007**, *129*, 12924–12925.
(2) Yuan, J. Y.; Xu, Y. Y.; Walther, A.; Bolisetty, S.; Schumacher, M.; Schmalz, H.; Ballauff, M.; Müller, A. H. E. *Nat. Mater.* **2008**, *7*, 718–722.
(3) Wang, H.; Patil, A. J.; Liu, K.; Petrov, S.; Mann, S.; Winnik, M. A.; Manners, I. *Adv. Mater.* **2009**, *21*, 1805–1808.
(4) Hartgerink, J. D.; Beniash, E.; Stupp, S. I. *Science* **2001**, *294*, 1684–1688.
(5) Silva, G. A.; Czeisler, C.; Niece, K. L.; Beniash, E.; Harrington, D. A.; Kessler, J. A.; Stupp, S. I. *Science* **2004**, *303*, 1352–1355.
(6) Tan, J. P. K.; Kim, S. H.; Nederberg, F.; Appel, E. A.; Waymouth, R. M.; Zhang, Y.; Hedrick, J. L.; Yang, Y. Y. *Small* **2009**, *5*, 1504–1507.
(7) Geng, Y.; Dalhaimer, P.; Cai, S. S.; Tsai, R.; Tewari, M.; Minko, T.; Discher, D. E. *Nat. Nanotechnol.* **2007**, *2*, 249–255.
(8) (a) Won, Y.-Y.; Davis, H. T.; Bates, F. S. *Science* **1999**, *283*, 960–963. (b) Wang, X. S.; Guerin, G.; Wang, H.; Wang, Y. S.; Manners, I.; Winnik, M. A. *Science* **2007**, *317*, 644–647. (c) Gädt, T.; Ieong, N. S.; Cambridge, G.; Winnik, M. A.; Manners, I. *Nat. Mater.* **2009**, *8*, 144–150.
(9) Cui, H. G.; Chen, Z. Y.; Zhong, S.; Wooley, K. L.; Pochan, D. J. *Science* **2007**, *317*, 647–650.
(10) Zhu, J. T.; Hayward, R. C. *J. Am. Chem. Soc.* **2008**, *130*, 7496–7502.
(11) Baram, J.; Shirman, E.; Ben-Shitrit, N.; Ustinov, A.; Weissman, H.; Pinkas, I.; Wolf, S. G.; Rybtchinski, B. *J. Am. Chem. Soc.* **2008**, *130*, 14966–14967.
(12) Hadjichristidis, N.; Iatrou, H.; Pispas, S.; Pitsikalis, M. *J. Polym. Sci., Part A: Polym. Chem.* **2000**, *38*, 3211–3234.
(13) Hong, L. Z.; Jin, F.; Li, J. F.; Lu, Y. J.; Wu, C. *Macromolecules* **2008**, *41*, 8220–8224.
(14) Jin, F.; Wu, C. *Acta Polym. Sin.* **2005**, 486–490.
(15) Tu, Y. F.; Wan, X. H.; Zhang, D.; Zhou, Q. F.; Wu, C. *J. Am. Chem. Soc.* **2000**, *122*, 10201–10205.
(16) LaRue, I.; Adam, M.; Pitsikalis, M.; Hadjichristidis, N.; Rubinstein, M.; Sheiko, S. S. *Macromolecules* **2006**, *39*, 309–314.
(17) Read, E. S.; Armes, S. P. *Chem. Commun.* **2007**, 3021–3035.

JA907898U